

Survival Analysis with Graph-Based Regularization for Predictors

Xi He^{*1}, Liyan Xie^{*†2}, Yao Xie¹, and Pinar Keskinocak¹

¹H. Milton Stewart School of Industrial and Systems Engineering

Georgia Institute of Technology

²School of Data Science

The Chinese University of Hong Kong, Shenzhen

August 31, 2021

Abstract

We study the variable selection problem in survival analysis to identify the most important factors affecting the survival time when the variables have prior knowledge that they have a mutual correlation through a graph structure. We consider the Cox proportional hazard model with a graph-based regularizer for variable selection. A computationally efficient algorithm is developed to solve the graph regularized maximum likelihood problem by connecting to group lasso. We provide theoretical guarantees about the recovery error and asymptotic distribution of the proposed estimators. The good performance and benefit of the proposed approach compared with existing methods are demonstrated in both synthetic and real data examples.

Keywords: Cox proportional hazard model, graphs regularizer, variable selection.

^{*}The first two authors contributed equally to the paper. Address correspondence to: Yao Xie, School of Industrial and Systems Engineering, Georgia Institute of Technology, Atlanta, Georgia, 30332, USA; E-mail: yao.xie@isye.gatech.edu.

[†]This work was done while the author was a graduate student in the School of Industrial and Systems Engineering, Georgia Institute of Technology.

1 Introduction

Variable selection is a fundamental problem in predictive modeling: when the feature vector is high-dimensional, it is important to select a subset of significant variables for model interpretation and predictability (Hastie et al., 2015). Variable selection arises in a wide range of applications, including genetics (Tachmazidou et al., 2010), healthcare (Newcombe et al., 2017; Duan et al., 2018), epidemiology (Greenland, 1989; Walter and Tiemeier, 2009), and so on. Variable selection is also of interest in survival analysis with high-dimensional covariates. For example, in organ transplantation, we are interested in knowing which variable is useful in predicting the post-transplant survival time of each patient. In such cases, efficient identification of the key variables will be useful for better decision-making. Variable selection has also been studied for survival analysis with ℓ_1 -regularization by Fan et al. (2010).

In various applications, variables are correlated, and the correlation structure can be modeled using a graph structure, e.g., from prior knowledge or pre-estimated. For instance, in medical problems, there can be certain correlation structures among the predicting variables (see, e.g., a real-data example illustrated in Fig. 1). When such knowledge is available, incorporating it in variable selection may help to achieve more precise results. Instead of selecting individual variables, whenever a variable is selected, its neighbors are likely to be selected as well (as a group of variables).

Motivated by this, in this paper, we study variable selection for survival analysis by developing a graph-based regularization survival model when the variables are correlated through a graph structure. We achieve this by considering the Cox proportional hazard model (Cox, 1972) with a graph regularizer to incorporate graph correlation structure between variables, in the presence of both complete observations and right-censored data. The graph is constructed from prior knowledge or estimating the correlation between predicting variables, represented as a graph $G = (V, E)$ where V and E are the node and edge set, respectively. A node $v \in V$ represents a predicting variable and an edge (u, v) connecting two nodes in the graph if the corresponding variables are correlated. We estimate the model parameter through the graph regularized maximum likelihood problem,

which can be solved efficiently by making a connection with group lasso (similar to the approach in Yu and Liu (2016)). We establish a performance guarantee for model recovery error and the asymptotic normality of the estimated parameter. The good performance of the proposed method and the benefit of graph regularization (compared with methods without considering the graph correlation structure among variables) is demonstrated using synthetic and real-data examples.

The rest of the paper is organized as follows. Section 1.1 reviews some existing work on regularization and variable selection for Cox proportional hazard model. Section 2 reviews the preliminaries on survival analysis and graph-based regularization. Section 3 presents the proposed regularization method for Cox model, together with discussions on efficient algorithms for solving the coefficients estimate based on a predictor duplication method. Section 4 contains the main theoretical results, including guarantees for the accuracy and consistency of the maximum regularized likelihood estimate. Section 5 contains numerical results comparing different methods using simulation. Section 6 presents the application of the proposed method to two real data examples: the pediatric kidney transplant data and the primary biliary cirrhosis sequential data, and compares performance with other regularization methods. Section 7 concludes the paper. All proofs and additional numerical details are delegated to the appendix.

1.1 Literature

Cox proportional hazard model is widely studied in survival analysis literature. We review some existing model selection and variable selection methods for Cox proportional hazard model. One line of work focus on the Bayesian variable selection procedures for censored survival data, by applying different prior distributions on the coefficients. In Faraggi and Simon (1997, 1998), the partial likelihood function is considered to avoid specifying the unknown baseline hazard function and a normal prior is used to estimate the regression coefficients. In Ibrahim et al. (1999), the full likelihood function is considered, and they specify a nonparametric prior for the baseline hazard and a parametric prior for the regression coefficients. In Giudici et al. (2003), the mixtures of products of Dirichlet process

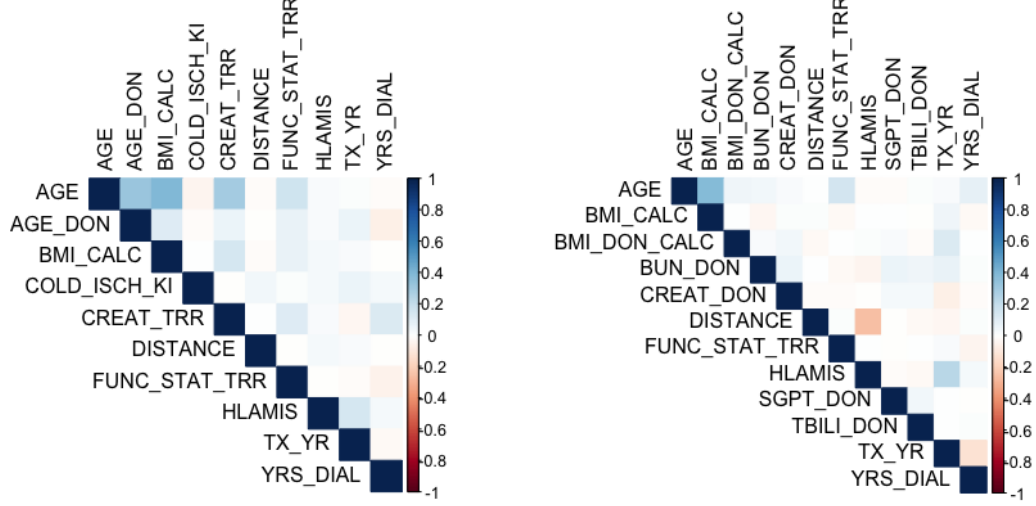


Figure 1: Graph structure for correlation of variables in a pediatric kidney transplant data set: the inverse covariance matrix of the numerical variables in the living donor dataset (left) and the deceased donor dataset (right); more details given in Section 6.

priors are used to compare the explanatory power of each covariate. In Lee et al. (2011), a special shrinkage prior based on normal and Gamma distributions is used to handle cases when the explanatory variables are of very high dimension. In Nikooienejad et al. (2020), a mixture prior is used which composed of a point mass at zero and an inverse moment prior. Other than using priors, a structure-based method using Bayesian networks is proposed in Lagani and Tsamardinos (2010) for variable selection as well.

Another line of work performs variable selection through regularization, i.e., adding a regularization term into the loss function or likelihood function. In Tibshirani (1997), the lasso regularization is applied for Cox proportional hazard model. In Fan and Li (2002), the Smoothly Clipped Absolute Deviation (SCAD) regularization is proposed, and the resulted estimate is shown to have oracle property, i.e., the resulting estimate can correctly identify the true model; see Fan et al. (2005) for an overview on such methods. In Wu (2012), the elastic net regularization is applied to the Cox model, and a solution path algorithm is developed; later in Khan and Shaw (2016), the adaptive elastic net is further applied for survival problems. In Chaturvedi et al. (2014), the fused lasso regularization is used,

with applications to genomics. In Zhang and Lu (2007), the adaptive lasso is applied, and the consistency and convergence results are provided. In survival applications involving categorical variables, the group lasso regularization (Yuan and Lin, 2006) is also often used, see Kim et al. (2012); Utazirubanda et al. (2019) for examples.

There is also much work on the variants of classical Cox regression problems. In Bradic et al. (2011), the regularization for Cox's proportional hazards model is studied for non-polynomial dimensional data. In Cai et al. (2008), the partially linear hazard regression with varying coefficients is studied. In Efron (2002), the two-way proportional hazards model is studied. In Kvamme et al. (2019), a time-to-event prediction framework is proposed using neural networks and Cox regression. In Rennert and Xie (2018), the Cox regression model is studied under dependent truncation.

Graph-based regression problems have been studied in Yu and Liu (2016), Li et al. (2020), Tibshirani et al. (2005). In this paper, we apply the graph-based regularization function to the Cox proportional hazard model and provide performance guarantees on the parameter estimate. This, to the best of our knowledge, is a new contribution to variable selection in survival analysis.

2 Preliminaries

2.1 Cox proportional hazard model

We first introduce the Cox model (Cox, 1972) in survival analysis. Denote T as the event time. Throughout the text, organ transplantation is used as an example to illustrate the models and methods, where T refers to the post-transplant survival time of a patient. Assume T is a random variable with cumulative distribution function (cdf) $F(t) = \mathbb{P}(T \leq t)$, and probability density function (pdf) $f(t) = F'(t) = dF(t)/dt$.

Define the event function as the upper tail probability:

$$S(t) = \mathbb{P}(T > t) = 1 - F(t).$$

The hazard function is defined as:

$$h(t) = \frac{f(t)}{S(t)} = -\frac{S'(t)}{S(t)} = -\frac{\partial}{\partial t} \log S(t). \quad (1)$$

Denote the cumulative hazard function as $H(t) = \int_0^t h(u)du$. By taking integral on both sides of (1), we have

$$S(t) = \exp\{-H(t)\}.$$

Data is given in the form $(y_1, \delta_1, \mathbf{x}_1), \dots, (y_n, \delta_n, \mathbf{x}_n)$, where y_i is the time until the event, $\delta_i = 1$ indicates a complete observation and $\delta_i = 0$ a right-censored observation, $\mathbf{x}_i = [x_{i1}, \dots, x_{ip}]^\top$ is the p -dimensional vector of predictors (covariates) for observation i , and n denotes the sample size. For simplicity, assume that there are no tied event times. In the organ transplant example, an observation is a transplant (patient-organ pair), \mathbf{x}_i includes patient and donor/organ characteristics, and no tied event times means that no two patients have the same post-transplant survival time.

Given $\{(y_i, \delta_i, \mathbf{x}_i)\}_{i=1}^n$, by the definition of hazard in (1), the likelihood function is

$$L(\{(y_i, \delta_i, \mathbf{x}_i)\}_{i=1}^n) = \prod_{i:\delta_i=1} f(y_i|\mathbf{x}_i) \prod_{i:\delta_i=0} S(y_i|\mathbf{x}_i) = \prod_{i:\delta_i=1} h(y_i|\mathbf{x}_i) \prod_{i=1}^n S(y_i|\mathbf{x}_i). \quad (2)$$

Throughout this paper, we utilize the Cox proportional hazard model (Cox, 1972) defined as follows. The hazard function at time t , given \mathbf{x}_i , takes the form

$$h(t|\mathbf{x}_i) = h_0(t) \exp(\boldsymbol{\beta}^\top \mathbf{x}_i), \quad (3)$$

where $h_0(\cdot)$ is the baseline hazard function, and $\boldsymbol{\beta} = [\beta_1, \dots, \beta_p]^\top$ is the vector of parameters to be estimated. Let $H_0(t) = \int_0^t h_0(u)du$. Then the cumulative hazard function can be written as $H(t|\mathbf{x}_i) = H_0(t) \exp(\boldsymbol{\beta}^\top \mathbf{x}_i)$, and we have:

$$S(y_i|\mathbf{x}_i) = \exp\{-H(y_i|\mathbf{x}_i)\} = \exp\{-H_0(y_i) \exp(\boldsymbol{\beta}^\top \mathbf{x}_i)\}. \quad (4)$$

Substitute (4) and (3) into the likelihood function (2) and take the log, we obtain the full log-likelihood function under parameter $\boldsymbol{\beta}$:

$$\ell(\boldsymbol{\beta}) = \sum_{i:\delta_i=1} [\log h_0(y_i) + \boldsymbol{\beta}^\top \mathbf{x}_i] - \sum_{i=1}^n H_0(y_i) \exp(\boldsymbol{\beta}^\top \mathbf{x}_i). \quad (5)$$

Our goal is to infer the unknown parameters $\boldsymbol{\beta}$ given observations $\{(y_i, \delta_i, \mathbf{x}_i)\}_{i=1}^n$. Taking the organ transplant as an example, we aim to identify the coefficients of patient and donor/organ characteristics that affect the post-transplant survival time.

2.2 Partial likelihood function

The baseline hazard function $h_0(\cdot)$ is usually unknown and has not been parameterized. Therefore, we adopt the commonly used partial likelihood function (Cox, 1975) instead of the full log-likelihood shown in (5). The partial likelihood function is defined as the probability of the event being observed for observation i at time y_i :

$$L_i(\boldsymbol{\beta}) = \frac{h(y_i | \mathbf{x}_i)}{\sum_{j:y_j \geq y_i} h(y_j | \mathbf{x}_j)} = \frac{\exp(\boldsymbol{\beta}^\top \mathbf{x}_i)}{\sum_{j:y_j \geq y_i} \exp(\boldsymbol{\beta}^\top \mathbf{x}_j)}.$$

Assuming independence of the observations, the joint partial likelihood function becomes

$$L(\boldsymbol{\beta}) = \prod_{i:\delta_i=1} L_i(\boldsymbol{\beta}) = \prod_{i:\delta_i=1} \frac{\exp(\boldsymbol{\beta}^\top \mathbf{x}_i)}{\sum_{j:y_j \geq y_i} \exp(\boldsymbol{\beta}^\top \mathbf{x}_j)},$$

and the partial log-likelihood is given by

$$\ell(\boldsymbol{\beta}) = \sum_{i=1}^n \delta_i \left\{ \boldsymbol{\beta}^\top \mathbf{x}_i - \log \left(\sum_{j:y_j \geq y_i} \exp(\boldsymbol{\beta}^\top \mathbf{x}_j) \right) \right\}. \quad (6)$$

Another interpretation of (6), as given in Fan and Li (2002), is to substitute the “least informative” nonparametric prior for the unknown baseline cumulative hazard $H_0(\cdot)$. We use the formulation (6) in the remainder of this paper.

2.3 Common regularization functions

The classical lasso-based method for the Cox model solves the optimization problem:

$$\min_{\boldsymbol{\beta}} -\frac{1}{n} \ell(\boldsymbol{\beta}) + g(\boldsymbol{\beta}), \quad (7)$$

where $\ell(\boldsymbol{\beta})$ is the partial log-likelihood function and $g(\boldsymbol{\beta})$ is the regularization term. A selected subset of potential representations for $g(\boldsymbol{\beta})$ include:

1. Lasso (Tibshirani, 1997): $g(\boldsymbol{\beta}) = \lambda \|\boldsymbol{\beta}\|_1$.

2. SCAD regularization (Fan and Li, 2002): $g(\boldsymbol{\beta}) = \sum_{j=1}^p f_\lambda(|\beta_j|)$, where $f'_\lambda(\theta) = \mathbb{1}(\theta \leq \lambda) + \frac{(a\lambda - \theta)_+}{(a-1)\lambda} \mathbb{1}(\theta > \lambda)$, $a > 2$, $\theta > 0$.
3. Elastic net (Wu, 2012): $g(\boldsymbol{\beta}) = \frac{\gamma}{2} \sum_{j=1}^p \beta_j^2 + \lambda \sum_{j=1}^p |\beta_j|$.
4. Fused lasso (Chaturvedi et al., 2014): $g(\boldsymbol{\beta}) = \lambda_1 \sum_{j=1}^p |\beta_j| + \lambda_2 \sum_{j=1}^{p-1} |\beta_{j+1} - \beta_j|$.
5. Adaptive lasso (Zhang and Lu, 2007): $g(\boldsymbol{\beta}) = \lambda \sum_{j=1}^p \tau_j |\beta_j|$ with positive weights τ_j .
6. Group lasso (Yuan and Lin, 2006): $g(\boldsymbol{\beta}) = \lambda \sum_{k=1}^p \|\boldsymbol{\beta}_{\mathcal{I}_k}\|_2$, where \mathcal{I}_k is the set of variables belonging to the k^{th} group.

It is worth mentioning that those classical regularization terms do not consider potential correlations between different predictors.

3 Graph-Based Regularization for Cox Model

Now we introduce the graph-based regularization given *known* or *pre-estimated* predictor graph for *correlated* variables in the Cox model. Let $X = (\mathbf{x}_1, \dots, \mathbf{x}_n)^\top = (X_1, \dots, X_p) \in \mathbb{R}^{n \times p}$, with X_1, \dots, X_p being column vectors and each column corresponds to a variable and its values across n observations (i.e., patient-organ pairs). Assume a known covariance structure among X_1, \dots, X_p . For instance, in the organ transportation data set detailed in Section 6.1, Figure 1 shows an example of the correlation between predicting variables. To represent such correlations among the predictors, we can construct an undirected and unweighted graph $G = (V, E)$ where V and E denote the nodes and edges, respectively. The graph can be constructed either by sample estimate or by domain knowledge. There is a node $i \in V$ for each variable i and an edge $(i, j) \in E$ if variables i and j are correlated. Let E_G be the matrix representing the edge set, where $E_G(i, j) = 1$ if $(i, j) \in E$ or $i = j$, and 0 otherwise. Let $\mathcal{N}_i = \{j : E_G(i, j) = 1\}$ denote the neighbors of node i and let $d_i = |\mathcal{N}_i|$ denote the cardinality of the set \mathcal{N}_i .

Before introducing our main optimization model, we first recall that our goal is to recover the decision variables $\boldsymbol{\beta}$ by solving a regularized optimization problem as shown in (7). The decision variables $\boldsymbol{\beta}$ corresponds to the coefficients for predictors (covariates). By

incorporating the additional correlation information on X (captured by the graph G), for a collection of non-negative weights $\boldsymbol{\tau} := \{\tau_1, \dots, \tau_p\}$, we now define a new norm of $\boldsymbol{\beta}$ as:

$$\|\boldsymbol{\beta}\|_{G, \boldsymbol{\tau}} := \min_{\sum_{k=1}^p V^{(k)} = \boldsymbol{\beta}, \text{ supp}(V^{(k)}) \subseteq \mathcal{N}_k} \sum_{k=1}^p \tau_k \|V^{(k)}\|_2. \quad (8)$$

Intuitively, the parameter $\boldsymbol{\beta}$ is decomposed into p terms. For the k -th predictor, the corresponding term $V^{(k)}$ characterizes the connection between the k -th predictor and its neighbors in the graph G , i.e., $V^{(k)}$ is only supported on \mathcal{N}_k , the neighboring set of node k . The parameter $\tau_k \geq 0$ is the regularization parameter that controls the importance of the regularization term $\|V^{(k)}\|_2$ for k -th predictor. It can be verified that $\|\boldsymbol{\beta}\|_{G, \boldsymbol{\tau}}$ satisfies the triangle inequality and is indeed a norm (Obozinski et al., 2011).

Let the regularization term in (7) be $g(\boldsymbol{\beta}) = \lambda \|\boldsymbol{\beta}\|_{G, \boldsymbol{\tau}}$ for a regularization constant $\lambda \geq 0$, then we find the parameter $\boldsymbol{\beta}$ by solving

$$\min_{\boldsymbol{\beta} \in \mathbb{R}^p} -\frac{1}{n} \sum_{i=1}^n \delta_i \left\{ \boldsymbol{\beta}^\top \mathbf{x}_i - \log \left(\sum_{j: y_j \geq y_i} \exp(\boldsymbol{\beta}^\top \mathbf{x}_j) \right) \right\} + \lambda \|\boldsymbol{\beta}\|_{G, \boldsymbol{\tau}},$$

which is also equivalent to

$$\begin{aligned} & \min_{\boldsymbol{\beta}, V^{(1)}, \dots, V^{(p)}} -\frac{1}{n} \sum_{i=1}^n \delta_i \left\{ \boldsymbol{\beta}^\top \mathbf{x}_i - \log \left(\sum_{j: y_j \geq y_i} \exp(\boldsymbol{\beta}^\top \mathbf{x}_j) \right) \right\} + \lambda \sum_{k=1}^p \tau_k \|V^{(k)}\|_2, \\ & \text{s.t.} \quad \sum_{k=1}^p V^{(k)} = \boldsymbol{\beta}, \quad \text{supp}(V^{(k)}) \subseteq \mathcal{N}_k, \quad \forall k. \end{aligned} \quad (9)$$

It is worth mentioning that the regularization term $\|\boldsymbol{\beta}\|_{G, \boldsymbol{\tau}}$ is very general, since it will be reduced to adaptive Lasso when there is no edge in the graph G , to group lasso when the graph G has several disconnected complete subgraphs, and reduced to ridge regression when the graph is a complete graph (Yu and Liu, 2016).

The optimization problem in (9) could be reformulated to an unconstrained convex problem such that it can be solved efficiently using existing solvers. This technique is developed based on the *predictor duplication* method proposed in Obozinski et al. (2011). For the observation \mathbf{x}_i and the k -th predictor, let $\mathbf{x}_{\mathcal{N}_k}^i$ be the $|\mathcal{N}_k| \times 1$ subvector of \mathbf{x}_i , with indices from \mathcal{N}_k . Similarly, let $V_{\mathcal{N}_k}^{(k)}$ be the $|\mathcal{N}_k| \times 1$ subvector of $V^{(k)}$. Recall that we have the constraint $\text{supp}(V^{(k)}) \subseteq \mathcal{N}_k$, thus the subvector $V_{\mathcal{N}_k}^{(k)}$ contains all non-zero values

of the vector $V^{(k)}$. Then $\sum_{i=1}^n \boldsymbol{\beta}^\top \mathbf{x}_i = \sum_{i=1}^n \sum_{k=1}^p V_{\mathcal{N}_k}^{(k)\top} \mathbf{x}_{\mathcal{N}_k}^i$, and the partial log-likelihood function in (6) can be rewritten as

$$\ell(\boldsymbol{\beta}) = \sum_{i=1}^n \delta_i \left\{ \sum_{k=1}^p V_{\mathcal{N}_k}^{(k)\top} \mathbf{x}_{\mathcal{N}_k}^i - \log \left(\sum_{j:y_j \geq y_i} \exp \left(\sum_{k=1}^p V_{\mathcal{N}_k}^{(k)\top} \mathbf{x}_{\mathcal{N}_k}^j \right) \right) \right\}. \quad (10)$$

Therefore, the optimization problem (9) reduces to the unconstrained optimization

$$\min_{V^{(1)}, \dots, V^{(p)}} -\frac{1}{n} \sum_{i=1}^n \delta_i \left\{ \sum_{k=1}^p V_{\mathcal{N}_k}^{(k)\top} \mathbf{x}_{\mathcal{N}_k}^i - \log \left(\sum_{j:y_j \geq y_i} \exp \left(\sum_{k=1}^p V_{\mathcal{N}_k}^{(k)\top} \mathbf{x}_{\mathcal{N}_k}^j \right) \right) \right\} + \lambda \sum_{k=1}^p \tau_k \|V_{\mathcal{N}_k}^{(k)}\|_2,$$

which can be solved using existing solvers for the group lasso regularization, such as the R package `grpreg` (Breheny, 2016). After obtaining the optimal solution to the above unconstrained problem, denoted as $\widehat{V}_{\mathcal{N}_k}^{(k)}$, $k = 1, \dots, p$, we let $\widehat{V}_{\mathcal{N}_k^c}^{(k)} = 0$ and the optimal parameter is $\widehat{\boldsymbol{\beta}} = \sum_{k=1}^p \widehat{V}^{(k)}$.

4 Theoretical Guarantees

In this section, we provide the theoretical properties for the estimate $\widehat{\boldsymbol{\beta}}$ solved from (9). We first introduce some useful notations. Denote $\boldsymbol{\beta}_0 = [\beta_{01}, \dots, \beta_{0p}]^\top$ as the true parameters (unknown), $J_0 = \{i : \beta_{0i} \neq 0\}$ is the index of non-zero parameters, $J_0^c = \{i : \beta_{0i} = 0\}$ is the index of zero parameters, and $s_0 = |J_0|$ denotes the number of non-zero parameters.

For any given $\boldsymbol{\beta}$ and a non-negative weights vector $\boldsymbol{\tau}$, we note that the norm $\|\boldsymbol{\beta}\|_{G, \boldsymbol{\tau}}$ of $\boldsymbol{\beta}$ as defined in (8) is computed based on the optimal decompositions $\{V^{(1)}, \dots, V^{(p)}\}$ of $\boldsymbol{\beta}$ such that $\boldsymbol{\beta} = \sum_{k=1}^p V^{(k)}$ and $\text{supp}(V^{(k)}) \subseteq \mathcal{N}_k$ for each k . Let $\mathcal{U}(\boldsymbol{\beta})$ denotes the set of all such decompositions of $\boldsymbol{\beta}$ that minimizes $\sum_{k=1}^p \tau_k \|V^{(k)}\|_2$. In other words, $\mathcal{U}(\boldsymbol{\beta})$ consists of all optimal solutions to the optimization problem (8):

$$\mathcal{U}(\boldsymbol{\beta}) = \left\{ \{V^{(1)}, \dots, V^{(p)}\} : \boldsymbol{\beta} = \sum_{k=1}^p V^{(k)}, \text{supp}(V^{(k)}) \subseteq \mathcal{N}_k, \sum_{k=1}^p \tau_k \|V^{(k)}\|_2 = \|\boldsymbol{\beta}\|_{G, \boldsymbol{\tau}} \right\}.$$

Denote $K_{G, \boldsymbol{\tau}}(\boldsymbol{\beta})$ as the minimum number of non-negative vectors among all optimal decompositions within the set $\mathcal{U}(\boldsymbol{\beta})$:

$$K_{G, \boldsymbol{\tau}}(\boldsymbol{\beta}) = \min_{\{V^{(1)}, \dots, V^{(p)}\} \in \mathcal{U}(\boldsymbol{\beta})} |\{i : \|V^{(i)}\|_2 \neq 0\}|,$$

and the constant $K_{G,\tau}$ is the supreme of $K_{G,\tau}(\beta)$ over all β satisfying $\text{supp}(\beta) \subseteq J_0$ (i.e., those that are consistent with the true parameter β_0):

$$K_{G,\tau} = \sup_{\text{supp}(\beta) \subseteq J_0} K_{G,\tau}(\beta).$$

We state two special cases to give an intuitive explanation for $K_{G,\tau}$, as presented in Yu and Liu (2016). In the first case, we assume the graph G has no edge, then we have $K_{G,\tau} = s_0$, since the constraint $\text{supp}(V^{(k)}) \subset \mathcal{N}_k = \{k\}$ now implies that the parameter $V^{(k)}$ can only have non-zero values on k -th entry, thus $K_{G,\tau}(\beta) = |\text{supp}(\beta)|$ for all β and the supreme of $K_{G,\tau}(\beta)$ is s_0 since $|J_0| = s_0$. In the second case, we assume G consists of K_0 disconnected complete subgraphs, where a complete subgraph is a subset of nodes in which all the nodes are connected to each other. Then we have $K_{G,\tau} = K_0$ and the set J_0 is the union of K_0 node sets of those disconnected complete subgraphs.

We adopt the same assumptions for the partial log-likelihood function as in Fan and Li (2002). Denote T, C, \mathbf{x} as the survival time, censoring time, and the associated covariates, respectively. Consider the general setting where the covariate may vary over time, denoted as $\mathbf{x}(t)$. The theory of counting process can be used to derive the theoretical guarantee for the resulted estimate. More specifically, define the counting process $N_i(t) = \mathbb{1}\{T_i \leq t, T_i \leq C_i\}$ and the indicator for being at risk $Y_i(t) = \mathbb{1}\{T_i \geq t, C_i \geq t\}$, where $\mathbb{1}\{\cdot\}$ is the indicator function. Without loss of generality, we only consider the time horizon $[0, 1]$. The results can be extended to interval $[0, \infty)$ (Andersen and Gill, 1982). Then the partial log-likelihood function in (6) can be rewritten by the counting process as:

$$\ell(\beta) = \sum_{i=1}^n \int_0^1 \beta^\top \mathbf{x}_i(t) dN_i(t) - \int_0^1 \log \left(\sum_{i=1}^n Y_i(t) \exp(\beta^\top \mathbf{x}_i(t)) \right) d\bar{N}(t),$$

where $dN_i(t)$ is the increment over infinitesimal interval $[t, t + dt)$ and it is either zero or one for the counting process N_i , $\bar{N} = \sum_{i=1}^n N_i$, and $d\bar{N}(t) = \sum_{i=1}^n dN_i(t)$.

Assumption 1 (Assumptions for the partial likelihood function (Fan and Li, 2002)). *Below, the expectation is taken with respect to $Y(t)$ which is a function of the random variable T , i.e., the survival time. We assume that:*

1. $\int_0^1 h_0(t) dt < \infty$.

2. The processes $\mathbf{x}(t)$ and $Y(t)$ are left-continuous with right hand limits, and

$$\mathbb{P}\{Y(t) = 1, \forall t \in [0, 1]\} > 0.$$

3. There exists a neighborhood $\mathcal{B} \subset \mathbb{R}^p$ of β_0 such that

$$\mathbb{E} \left\{ \sup_{t \in [0, 1], \beta \in \mathcal{B}} Y(t) \mathbf{x}(t)^\top \mathbf{x}(t) \exp\{\beta^\top \mathbf{x}(t)\} \right\} < \infty.$$

4. Define

$$\begin{aligned} s^{(0)}(\beta, t) &= \mathbb{E} [Y(t) \exp\{\beta^\top \mathbf{x}(t)\}], \\ s^{(1)}(\beta, t) &= \mathbb{E} [Y(t) \mathbf{x}(t) \exp\{\beta^\top \mathbf{x}(t)\}], \\ s^{(2)}(\beta, t) &= \mathbb{E} [Y(t) \mathbf{x}(t) \mathbf{x}(t)^\top \exp\{\beta^\top \mathbf{x}(t)\}], \end{aligned}$$

where $s^{(0)}(\cdot, t)$, $s^{(1)}(\cdot, t)$, $s^{(2)}(\cdot, t)$ are continuous in $\beta \in \mathcal{B}$, uniformly in $t \in [0, 1]$; $s^{(0)}, s^{(1)}, s^{(2)}$ are bounded on $\mathcal{B} \times [0, 1]$; $s^{(1)}$ is bounded away from zero on $\mathcal{B} \times [0, 1]$.

The matrix

$$I(\beta_0) = \int_0^1 \left(\frac{s^{(2)}(\beta_0, t)}{s^{(0)}(\beta_0, t)} - \left(\frac{s^{(1)}(\beta_0, t)}{s^{(0)}(\beta_0, t)} \right) \left(\frac{s^{(1)}(\beta_0, t)}{s^{(0)}(\beta_0, t)} \right)^\top \right) s^{(0)}(\beta_0, t) h_0(t) dt$$

is finite positive definite.

The reason of imposing the above assumptions is to obtain the local asymptotic quadratic property for the partial likelihood function $\ell(\beta)$, as well as the asymptotic normality of the maximum partial likelihood estimates (Andersen and Gill, 1982; Murphy and Van der Vaart, 2000).

We also make the following assumptions for the true predictor graph G which represents the underlying correlated structure among all predictors.

Assumption 2 (Assumptions for the predictor graph G). *The following assumptions are required for the true graph G :*

1. The neighborhood $\mathcal{N}_k \subseteq J_0$, $\forall k \in J_0$.

2. There exists $\kappa > 0$ such that

$$\inf_{\beta \in \mathbb{R}^p \setminus \{0\}, |J| \leq s_0} \inf_{\substack{(V^{(1)}, V^{(2)}, \dots, V^{(p)}) \in \mathcal{U}(\beta) \\ \sum_{k \notin J} \tau_k \|V^{(k)}\|_2 \leq \sum_{k \in J} \tau_k \|V^{(k)}\|_2}} \frac{\frac{1}{2} (\sum_{k=1}^p V^{(k)})^\top I(\beta_0) (\sum_{k=1}^p V^{(k)})}{\sum_{k \in J} \tau_k^2 \|V^{(k)}\|_2^2} \geq \kappa,$$

where β_0 is the true parameter.

Remark. The Assumption 2 (1) assumes that the predicted graph G is consistent with the true parameter β_0 , the same as the assumption (A2) in Yu and Liu (2016). The Assumption 2 (2) serves a similar role as the restricted eigenvalue condition for Lasso (Bickel et al., 2009) for proving the oracle properties of the estimate. Compared with the assumption (A3) for the data matrix in Yu and Liu (2016), here the assumption is for the Fisher information matrix, due to a different loss function, $-l(\beta)$, considered here.

Under the assumptions above, we present the recovery error for the maximum regularized likelihood estimate $\hat{\beta}$ and the difference between partial likelihood functions evaluated at $\hat{\beta}$ and true parameter β_0 , as summarized in Theorem 1.

Theorem 1 (Finite sample bounds). *Under the Assumptions 1 and 2, let $\tau_{\min} = \min_{1 \leq i \leq p} \tau_i$. For any optimal solution $\hat{\beta}$ of problem (9), we have*

$$\frac{1}{n} \left\{ \ell(\beta_0) - \ell(\hat{\beta}) \right\} \leq \frac{\lambda^2 K_{G,\tau}}{\kappa}, \quad \|\hat{\beta} - \beta_0\|_2 \leq \frac{2\lambda K_{G,\tau}}{\kappa \tau_{\min}}.$$

Theorem 1 shows that the recovery error $\|\hat{\beta} - \beta_0\|_2$ may be large when the smallest restricted eigenvalue κ as imposed in Assumption 2 (2) is close to zero, and the recovery error tends to be small when the regularizer parameter λ is small (note that $\lambda = 0$ results in the maximum likelihood estimate), and when τ_{\min} is large and the constant $K_{G,\tau}$ is small.

We also derive the asymptotic normality property of the maximum regularized likelihood estimate, under the case that the dimension p of covariate is fixed. We adopt the convention that β_{J_0} , $\beta_{J_0^c}$ denote the subvectors of β consisting of entries with index belong to the set J_0 and J_0^c , respectively, and $I_{J_0}(\beta_0)$ denotes the square matrix with rows and columns belong to the set J_0 .

Theorem 2 (Asymptotic normality). *When dimension p is fixed, assume $\sqrt{n}\lambda \rightarrow 0$ and $\tau_j = O(1)$ for each $j \in J_0$, $n^{(\gamma+1)/2}\lambda \rightarrow \infty$, and $\liminf_{n \rightarrow \infty} n^{-\gamma/2}\tau_j > 0$ for each $j \in J_0^c$,*

under Assumptions 2 (1), we have as $n \rightarrow \infty$,

$$\sqrt{n}(\widehat{\boldsymbol{\beta}}_{J_0} - \boldsymbol{\beta}_{0,J_0}) \xrightarrow{d} N(0, I_{J_0}(\boldsymbol{\beta}_0)^{-1}), \quad \widehat{\boldsymbol{\beta}}_{J_0^c} \xrightarrow{d} 0.$$

The results in Theorem 2 indicates that the proposed estimate is asymptotically consistent when the dimension p is fixed, in the sense that the support of the true parameter can be recovered. It also provides approximate confidence intervals for the estimate when the sample size is moderately large, based on the asymptotic normal distribution.

5 Simulation Study

To evaluate the performance of the graph regularizer for the Cox model, it is compared with some existing regularizers for the Cox model, including the classical lasso (Tibshirani, 1996, 1997), ridge regression (Hoerl and Kennard, 1970), elastic net (Zou and Hastie, 2005; Wu, 2012), SCAD (Fan and Li, 2001, 2002), and adaptive lasso (Alasso) (Zou, 2006; Zhang and Lu, 2007), see Section 2.3 for details.

The regularized survival models are evaluated on the following performance measures:

(i) ℓ_2 error of the estimated coefficients: $\|\widehat{\boldsymbol{\beta}} - \boldsymbol{\beta}_0\|_2$;

(ii) Relative prediction error (RPE):

$$RPE = \frac{1}{N_{\text{test}}}(\widehat{\boldsymbol{\beta}} - \boldsymbol{\beta}_0)^\top X_{\text{test}}^\top X_{\text{test}}(\widehat{\boldsymbol{\beta}} - \boldsymbol{\beta}_0),$$

where N_{test} is the test data size and $X_{\text{test}} \in \mathbb{R}^{N_{\text{test}} \times p}$ are the test covariates;

(iii) Harrell's concordance index (c-index) (Harrell Jr et al., 1996). The c-index is a commonly used metric for evaluating survival prediction models. It measures the ability of the model to correctly predict the ranking of the survival time given a pair of new observations and is equivalent to the Area Under Curve (AUC) (Huang and Ling, 2005). A c-index of 0.5 is equivalent to random guessing and 1 is perfect prediction. In recent survival applications, a c-index between 0.6 and 0.7 is often considered satisfactory (Laimighofer et al., 2016).

Three types of predictor graph topologies are tested in the simulation study: (1) the sparse graph, (2) the ring graph, and (3) the graph with communities. Figure 2 illustrates the corresponding graph typologies.

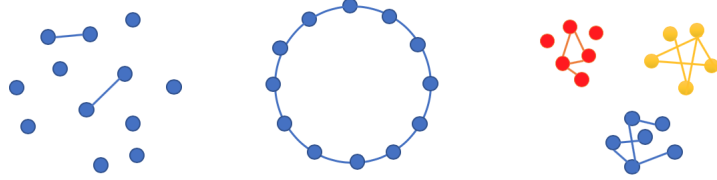


Figure 2: Illustration of three predictor graph typologies used in the simulation. From left to right: the sparse graph, the ring graph, and the graph with three communities.

In the following, we show that the proposed graph regularizer has overall the most promising performance among the regularizers for the Cox model that are tested in the simulation study.

5.1 The sparse graph

Consider a sparse Erdős-Rényi predictor graph with a small edge formation probability p_0 . Assume Gaussian distribution for the predictors: $(X_1, X_2, \dots, X_p)^\top \sim N(0, \Omega^{-1})$, where $p = 100$ and Ω is an inverse covariance matrix whose off-diagonal entries equal 0.5 with probability p_0 and 0 with probability $1 - p_0$. In practice, we compute $\Lambda = \Omega^{-1}$ using the *nearPD* transformation in the R package `matrix` (Bates et al., 2017) to ensure that Λ is positive definite. Let the true parameters be $\beta_0 = \Omega \Lambda_{xy}$, where $\Lambda_{xy} = (c_1, c_2, \dots, c_p)^\top$. Let $c_i = 10$ for the top 4 predictors with maximum edges, and $c_i = 0$ otherwise. The survival time is simulated using the R package `coxed` (Kropko and Jeffrey, 2019) with a censor rate of 0.3. The training size is 100 and the testing size is 400. The hyper-parameters in each model are tuned by cross-validation using the training data.

The experiment is repeated 50 times, and the results (mean and standard deviation) of the models are shown in Table 1, 2, and 3 for $p_0 = 0.01, 0.05, 0.1$, respectively. We see that the proposed method based on graph regularizer results in lower ℓ_2 error and RPE, and higher c-index, compared to other regularizers and baseline models, regardless of the edge

formation probability (see Table 1, 2, 3). As the edge formation probability p_0 increases, the performance of all models gets worse, but the graph-based regularization consistently results in better prediction than other models.

Table 1: Performance on the sparse Erdős-Rényi predictor graph, $p_0 = 0.01$.

| Model | ℓ_2 norm | RPE | c-index |
|----------------------------|---------------------|---|---------------------|
| Graph regularizer | 28.73 (0.39) | 415.98 (28.90) | 0.74 (0.042) |
| Lasso | 30.29(0.12) | 501.58(29.52) | 0.66(0.042) |
| Ridge regression | 30.37(0.34) | 504.85(29.59) | 0.60(0.023) |
| Elastic net | 30.30(0.084) | 502.24(29.71) | 0.66(0.042) |
| SCAD | 30.33(0.088) | 503.29(29.75) | 0.66(0.048) |
| Alasso | 30.40(0.016) | 505.69(29.64) | 0.62(0.074) |
| $\hat{\beta} = \mathbf{0}$ | 30.41(0.00) | 506.34(29.70) | 0.50(0.00) |
| Cox without regularization | Inf(-) | 7.54×10^7 (4.00×10^8) | 0.53(0.044) |

Table 2: Performance on the sparse Erdős-Rényi predictor graph, $p_0 = 0.05$.

| Model | ℓ_2 norm | RPE | c-index |
|----------------------------|---------------------|---|---------------------|
| Graph regularizer | 41.94 (0.46) | 576.57 (50.28) | 0.70 (0.034) |
| Lasso | 42.28(0.15) | 585.81(49.80) | 0.68(0.034) |
| Ridge regression | 42.37(0.052) | 589.49(50.06) | 0.66(0.034) |
| Elastic net | 42.27(0.15) | 585.59(50.79) | 0.67(0.033) |
| SCAD | 42.37(0.092) | 589.25(49.98) | 0.68(0.048) |
| Alasso | 42.43(0.020) | 590.93(50.03) | 0.62(0.06) |
| $\hat{\beta} = \mathbf{0}$ | 42.41(0.00) | 591.73(50.11) | 0.50(0.00) |
| Cox without regularization | Inf(-) | 5.04×10^8 (1.59×10^9) | 0.57(0.054) |

5.2 The ring graph

The second experiment is on a ring predictor graph where the variables are nodes on the ring and each node is connected to its immediate two neighbors. Let $(X_1, X_2, \dots, X_p)^\top \sim N(0, \Omega^{-1})$, where $p = 100$. Let $\Omega = B + \delta I_p$, where $B_{ij} = 0.5$ for $|i - j| < 2$ and $B_{ii} = 0$, I_p

Table 3: Performance on the sparse Erdős-Rényi predictor graph, $p_0 = 0.1$.

| Model | ℓ_2 norm | RPE | c-index |
|----------------------------|---------------------|--|---------------------|
| Graph regularizer | 59.99 (0.55) | 869.37 (58.42) | 0.70 (0.034) |
| Lasso | 60.46(0.19) | 885.81(58.62) | 0.68(0.033) |
| Ridge regression | 60.57(0.055) | 890.19(58.15) | 0.66(0.032) |
| Elastic net | 60.47(0.15) | 886.21(58.73) | 0.68(0.033) |
| SCAD | 60.57(0.058) | 889.94(58.00) | 0.67(0.039) |
| Alasso | 60.60(0.025) | 891.45(58.00) | 0.61(0.064) |
| $\hat{\beta} = \mathbf{0}$ | 60.62(0.00) | 892.38(57.97) | 0.50(0.00) |
| Cox without regularization | Inf(-) | 5.54×10^9 (2.70×10^{10}) | 0.54(0.049) |

is the identity matrix, and δ is chosen to make the condition number of Ω equal to p . Let the true parameter $\beta_0 = \Omega\mathbf{1}$, where $\mathbf{1} \in \mathbb{R}^{p \times 1}$ is a vector with all one entries.

From the results in Table 4, we observe that the graph-based regularizer has the best performance on the ℓ_2 norm, the RPE, and the c-index when the predictor graph is a ring graph. The competing models have close performance with the graph regularizer since the relations among the variables in the ring graph are relatively simple.

Table 4: Performance on the ring predictor graph.

| Model | ℓ_2 norm | RPE | c-index |
|----------------------------|---------------------|---|---------------------|
| Graph regularizer | 23.82 (0.23) | 232.78 (16.62) | 0.68 (0.032) |
| Lasso | 23.98(0.045) | 235.41(16.03) | 0.66(0.035) |
| Ridge regression | 23.97(0.037) | 235.24(16.14) | 0.66(0.038) |
| Elastic net | 23.96(0.083) | 235.17(16.35) | 0.66(0.035) |
| SCAD | 24.00(0.0092) | 235.65(16.00) | 0.61(0.034) |
| Alasso | 24.00(0.0039) | 235.68(16.03) | 0.55(0.040) |
| $\hat{\beta} = \mathbf{0}$ | 24.00(0.00) | 235.70(16.03) | 0.50(0.00) |
| Cox without regularization | Inf(-) | 2.07×10^5 (3.60×10^5) | 0.55(0.044) |

5.3 The graph with communities

Suppose some of the predictors have community identities, and for predictors in the same community, an edge forms with probability p_{in} ; for predictors in different communities or those not in any communities, let the probability of edge formation among them be p_{out} . Let $p_{\text{in}} = 0.5, 0.7, 0.9$, and $p_{\text{out}} = 0.01$. For dimension $p = 100$, we assume there exist three communities, each with size 30.

The performance comparison is shown in Table 5, 6, and 7 for $p_{\text{in}} = 0.5, 0.7$, and 0.9, respectively. We observe that the graph-based regularization has the best ℓ_2 norm and c-index regardless of the value of p_{in} . As p_{in} increases, the communities become more dense, and the relations among the variables become more complex. Therefore, it becomes more difficult for the models to acquire accurate estimation and prediction.

Table 5: Performance on the 3-community predictor graph, $p_{\text{in}} = 0.5$.

| Model | ℓ_2 norm | RPE | c-index |
|----------------------------|--------------------|---------------------------------------|--------------------|
| Graph regularizer | 59.80(0.75) | 746.56(78.63) | 0.70(0.036) |
| Lasso | 60.56(0.058) | 770.61(77.78) | 0.66(0.031) |
| Ridge regression | 60.60(0.029) | 772.13(76.88) | 0.64(0.034) |
| Elastic net | 60.55(0.081) | 769.99(77.67) | 0.66(0.032) |
| SCAD | 60.60(0.028) | 772.26(77.00) | 0.64(0.036) |
| Alasso | 60.62(0.0057) | 773.20(76.98) | 0.57(0.043) |
| $\hat{\beta} = \mathbf{0}$ | 60.62(0.00) | 773.48(76.91) | 0.50(0.00) |
| Cox without regularization | Inf(-) | $1.40 \times 10^6 (5.16 \times 10^6)$ | 0.54(0.055) |

6 Real Data Examples

We apply the graph-based regularizer on two real datasets: the pediatric kidney transplant data and the primary biliary cirrhosis sequential (pbcsseq) data, and compare performance with other commonly used regularization methods.

Table 6: Performance on the 3-community predictor graph, $p_{\text{in}} = 0.7$.

| Model | ℓ_2 norm | RPE | c-index |
|----------------------------|---------------------|---|---------------------|
| Graph regularizer | 77.74 (0.53) | 737.92(43.31) | 0.70 (0.044) |
| Lasso | 78.40(0.035) | 734.13 (41.24) | 0.64(0.044) |
| Ridge regression | 78.40(0.024) | 734.50(41.13) | 0.62(0.038) |
| Elastic net | 78.40(0.028) | 734.25(41.16) | 0.64(0.043) |
| SCAD | 78.41(0.026) | 734.72(41.09) | 0.61(0.040) |
| Alasso | 78.42(0.0041) | 735.14(40.98) | 0.54(0.038) |
| $\hat{\beta} = \mathbf{0}$ | 78.42(0.00) | 735.27(40.96) | 0.50(0.00) |
| Cox without regularization | Inf(-) | 1.81×10^6 (1.03×10^7) | 0.55(0.051) |

 Table 7: Performance on the 3-community predictor graph, $p_{\text{in}} = 0.9$.

| Model | ℓ_2 norm | RPE | c-index |
|----------------------------|---------------------|---|---------------------|
| Graph regularizer | 90.06 (0.43) | 875.48(88.090) | 0.68 (0.041) |
| Lasso | 90.55(0.017) | 834.60(60.21) | 0.611(0.037) |
| Ridge regression | 90.55(0.0094) | 834.54(60.27) | 0.55(0.027) |
| Elastic net | 90.55(0.020) | 834.48 (60.10) | 0.61(0.038) |
| SCAD | 90.55(0.0076) | 834.71(60.25) | 0.55(0.029) |
| Alasso | 90.55(0.0016) | 834.84(60.19) | 0.53(0.038) |
| $\hat{\beta} = \mathbf{0}$ | 90.55(0.00) | 834.87(60.19) | 0.50(0.00) |
| Cox without regularization | Inf(-) | 2.80×10^8 (1.61×10^9) | 0.54(0.045) |

6.1 The pediatric kidney transplant data

Predicting the survival time for transplant recipients is a crucial task for the transplant community. Accurate post-transplant survival prediction can provide helpful information for organ allocation decisions. A challenge with transplant survival prediction is that the data recorded for each transplant case are usually high-dimensional and highly correlated. Therefore, building a predictor graph and using the graph regularizer can be especially beneficial for solving the variable selection problems when building survival prediction models.

We use the proposed graph regularized Cox model to predict the survival time of pe-

diatric recipients of kidney transplantation. The dataset we use contains 19,236 pediatric kidney transplant cases in the U.S. from 1987 to 2014, and for each transplant case, there are 487 predictors. The dataset is provided by UNOS (United Network for Organ Sharing).

The donor type, i.e., living versus deceased, can significantly impact the post-transplant survival (Gjertson and Cecka, 2001; Terasaki et al., 1995); hence, we separate the observations into two data sets and develop corresponding regularized Cox models for observations with living and deceased donors, respectively.

We construct the predictor graph by connecting numerical predictors with high inverse covariance and connecting the paired categorical variables between the transplant recipient and the donor. For example, we connect the variable “HBV: positive” (recipient HBV infection status: positive) and “HBV_DON: positive” (donor HBV infection status: positive). This connection is based on the assumption that being in a similar condition as the donor is beneficial for the organ recipient’s post-transplant survivability.

Table 8: The performance of different methods on the pediatric kidney transplant data.

| Model | Living donors c-index | Deceased donors c-index |
|----------------------------|-----------------------|-------------------------|
| Graph regularizer | 0.59(0.045) | 0.58(0.055) |
| Lasso | 0.57(0.039) | 0.57(0.055) |
| Ridge regression | 0.49(0.039) | 0.56(0.060) |
| Elastic net | 0.57(0.038) | 0.58(0.045) |
| SCAD | 0.57(0.028) | 0.57(0.056) |
| Alasso | 0.57(0.040) | 0.57(0.049) |
| Group lasso | 0.57(0.051) | 0.57(0.038) |
| Cox without regularization | 0.49(0.039) | 0.55(0.058) |
| $\hat{\beta} = \mathbf{0}$ | 0.50(0.00) | 0.50(0.00) |

The performance of the graph regularized Cox model is compared with other regularizers in Table 8 and Figures 3. Since the true parameters are unknown in the real data, we only compare the c-index. We observe that the graph-based regularizer has the highest mean and median c-index for both donor types. The improvement of using the graph regularizer is more prominent on the living donor dataset. This result is possible due to the fact that

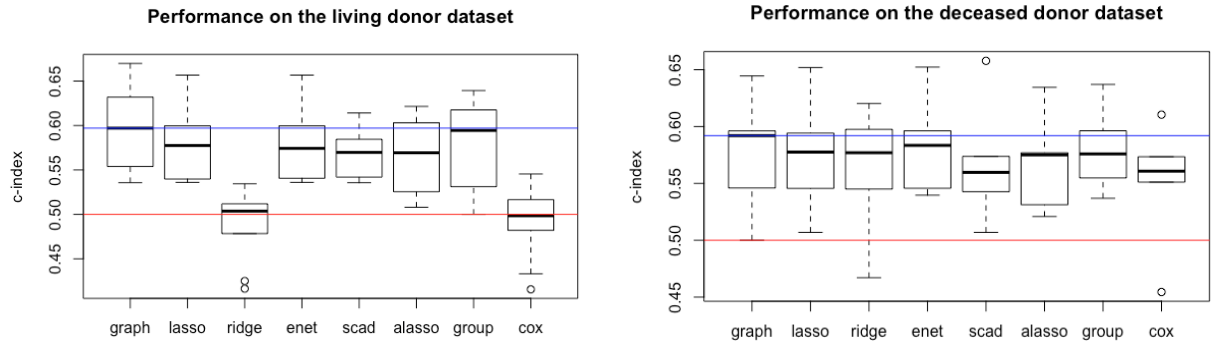


Figure 3: The boxplot of the model c-indices on the living (left) and deceased (right) donor datasets. Blue line indicates the median c-index of the proposed method; red line indicates where c-index equals to 0.5 (random guessing).

the living donor is more often related to the recipient and is likely to have closer biological and environmental characteristics as the recipient. More variables are also recorded from the living donors than from the deceased donors in the dataset. Therefore, the living donor predictor graph we can create is more complicated than the deceased donor’s, which gives the graph-based regularizer more advantage over other methods in predicting the survival outcome for pediatric recipients of living donor kidneys.

6.2 The primary biliary cirrhosis sequential (*pbcsq*) data

The *pbcsq* data (Murtaugh et al., 1994; Fleming and Harrington, 2011) in the R package **survival** (Therneau et al., 2020) is recorded by the Mayo Clinic to study the primary biliary cirrhosis (PBC) of the liver from 1974 to 1984. It contains the information of 1945 patients and 17 predicting variables.

To create a predictor graph, we analyze the relations of the variables in the *pbcsq* dataset. For the numerical variables, we compute their inverse covariance (shown in Figure 4). We connect pairs of variables if their Pearson’s test *p*-value is less than 0.05 (Kim, 2015). For the categorical variables, we connect variables representing different levels under the same categorical variable. For completeness, we summarize the variable relations for the predictor graph in Table 10 in the Appendix. The neighbors of a variable are those

that are connected to the variable.

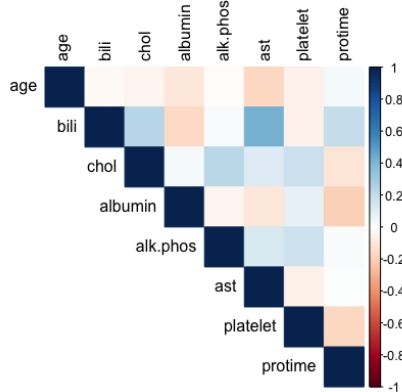


Figure 4: Inverse covariance of the numerical variables in the *pbcsq* dataset.

We compare the performance of the graph regularization to other methods using 10-fold cross-validation on the *pbcsq* dataset. Since this is a real data problem and the true parameters are unknown, only the c-index can be computed. The results are shown in Table 9 and Figure 5, where the blue reference line in the figure is the median of the graph lasso c-index.

As shown in Table 9, the graph-based regularizer has the highest c-index on the *pbcsq* dataset. The ridge regression, the elastic net, and the SCAD penalties also have good performance. The boxplot shows that the graph-based regularization has the highest median c-index. The ridge regression and the elastic net have about the same median c-index as the graph regularizer, but their distributions of the c-index are lower than the graph lasso.

Therefore, we can conclude that the graph-based regularization has satisfactory performance on the *pbcsq* dataset, although its performance improvement is limited by the fact that the problem is not high-dimensional ($p = 17$) and the graphical structure among the variables is relatively simple.

7 Conclusion and Discussions

In this paper, we have applied the graph-based regularization for Cox proportional hazard model to perform parameter estimation and variable selection. The graph-based regu-

Table 9: The performance of different penalties on the *pbcsseq* dataset.

| Model | c-index |
|----------------------------|--------------------|
| Graph regularizer | 0.88(0.086) |
| Lasso | 0.86(0.082) |
| Ridge regression | 0.87(0.092) |
| Elastic net | 0.87(0.085) |
| SCAD | 0.87(0.079) |
| Alasso | 0.86(0.088) |
| Group lasso | 0.86(0.076) |
| Cox without regularization | 0.83(0.098) |
| $\hat{\beta} = \mathbf{0}$ | 0.50(0.00) |

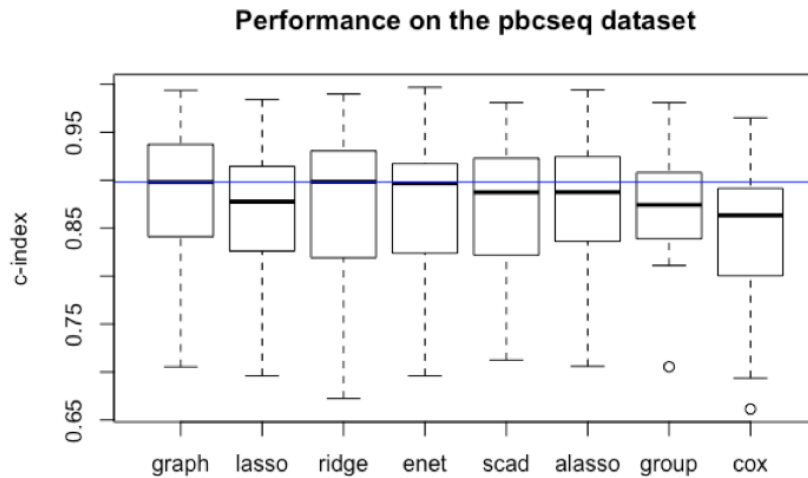


Figure 5: The boxplot of the model c-indices on the *pbcsseq* dataset. Blue line indicates the median c-index of the proposed method.

larization enables more accurate variable selection by considering the underlying graph structured correlation between different variables, as compared to existing methods without considering the graphical structure. Although the problem is motivated by the organ transplantation application, the proposed method is very general and applicable to other

applications such as sensor networks and social networks. Simulation studies and real data examples both demonstrate the promising performance of the proposed method under many different settings.

There are several related extensions that are worth consideration in future work. First, the choice of the regularization parameters λ and τ are critical to variable selection since there is typically a trade-off between sparsity and accuracy. Therefore, it would be useful to study the cross-validation for the Cox model under graph-based regularization, especially when we have censored data. The corresponding theoretical development is worth further investigation. Second, the graph structure used in this paper is for predicting variables only. We can also consider possible networks between donors and recipients for specific applications, such as the organ transplantation problem. Moreover, the graph can be further generalized to weighted graphs where weights may indicate the probability of success between each pair or the correlation of each pair of predicting variables.

Acknowledgement

The authors are grateful to Professor Guan Yu for helpful discussions. The authors gratefully acknowledge the support from NSF CAREER Award CCF-1650913, and NSF CMMI-2015787, DMS-1938106, DMS-1830210, and the Carlos and Marguerite Mason Trust Foundation and the Laura and John Arnold Foundation.

References

Andersen, P. K. and R. D. Gill (1982). Cox's regression model for counting processes: A large sample study. *Annals of Statistics* 10(4), 1100–1120.

Bates, D., M. Maechler, and M. M. Maechler (2017). Package ‘matrix’.

Bickel, P. J., Y. Ritov, and A. B. Tsybakov (2009). Simultaneous analysis of lasso and dantzig selector. *Annals of Statistics* 37(4), 1705–1732.

Bradic, J., J. Fan, and J. Jiang (2011). Regularization for Cox’s proportional hazards model with NP-dimensionality. *Annals of Statistics* 39(6), 3092–3120.

Breheny, P. (2016). Package ‘grpreg’.

Cai, J., J. Fan, J. Jiang, and H. Zhou (2008). Partially linear hazard regression with varying coefficients for multivariate survival data. *Journal of the Royal Statistical Society: Series B (Statistical Methodology)* 70(1), 141–158.

Chaturvedi, N., R. X. de Menezes, and J. J. Goeman (2014). Fused lasso algorithm for Cox proportional hazards and binomial logit models with application to copy number profiles. *Biometrical Journal* 56(3), 477–492.

Cox, D. R. (1972). Regression models and life-tables. *Journal of the Royal Statistical Society: Series B (Methodological)* 34(2), 187–202.

Cox, D. R. (1975). Partial likelihood. *Biometrika* 62(2), 269–276.

Duan, W., R. Zhang, Y. Zhao, S. Shen, Y. Wei, F. Chen, and D. C. Christiani (2018). Bayesian variable selection for parametric survival model with applications to cancer omics data. *Human Genomics* 12(1), 1–15.

Efron, B. (2002). The two-way proportional hazards model. *Journal of the Royal Statistical Society: Series B (Statistical Methodology)* 64(4), 899–909.

Fan, J., Y. Feng, Y. Wu, et al. (2010). High-dimensional variable selection for Cox’s proportional hazards model. In *Borrowing Strength: Theory Powering Applications—A Festschrift for Lawrence D. Brown*, pp. 70–86. Institute of Mathematical Statistics.

Fan, J., G. Li, and R. Li (2005). An overview on variable selection for survival analysis. *Contemporary Multivariate Analysis And Design Of Experiments: In Celebration of Professor Kai-Tai Fang’s 65th Birthday*, 315–336.

Fan, J. and R. Li (2001). Variable selection via nonconcave penalized likelihood and its oracle properties. *Journal of the American statistical Association* 96(456), 1348–1360.

Fan, J. and R. Li (2002). Variable selection for Cox's proportional hazards model and frailty model. *Annals of Statistics* 30(1), 74–99.

Faraggi, D. and R. Simon (1997). Large sample Bayesian inference on the parameters of the proportional hazard models. *Statistics in Medicine* 16(22), 2573–2585.

Faraggi, D. and R. Simon (1998). Bayesian variable selection method for censored survival data. *Biometrics* 54(4), 1475–1485.

Fleming, T. R. and D. P. Harrington (2011). *Counting Processes and Survival Analysis*, Volume 169. John Wiley & Sons.

Giudici, P., M. Mezzetti, and P. Muliere (2003). Mixtures of products of Dirichlet processes for variable selection in survival analysis. *Journal of Statistical Planning and Inference* 111(1-2), 101–115.

Gjertson, D. W. and J. M. Cecka (2001). Determinants of long-term survival of pediatric kidney grafts reported to the united network for organ sharing kidney transplant registry. *Pediatric Transplantation* 5(1), 5–15.

Greenland, S. (1989). Modeling and variable selection in epidemiologic analysis. *American Journal of Public Health* 79(3), 340–349.

Harrell Jr, F. E., K. L. Lee, and D. B. Mark (1996). Multivariable prognostic models: Issues in developing models, evaluating assumptions and adequacy, and measuring and reducing errors. *Statistics in Medicine* 15(4), 361–387.

Hastie, T., R. Tibshirani, and M. Wainwright (2015). *Statistical Learning with Sparsity: The Lasso and Generalizations*. CRC press.

Hoerl, A. E. and R. W. Kennard (1970). Ridge regression: Biased estimation for nonorthogonal problems. *Technometrics* 12(1), 55–67.

Huang, J. and C. X. Ling (2005). Using AUC and accuracy in evaluating learning algorithms. *IEEE Transactions on Knowledge and Data Engineering* 17(3), 299–310.

Ibrahim, J. G., M.-H. Chen, and S. N. MacEachern (1999). Bayesian variable selection for proportional hazards models. *Canadian Journal of Statistics* 27(4), 701–717.

Khan, M. H. R. and J. E. H. Shaw (2016). Variable selection for survival data with a class of adaptive elastic net techniques. *Statistics and Computing* 26(3), 725–741.

Kim, J., I. Sohn, S.-H. Jung, S. Kim, and C. Park (2012). Analysis of survival data with group lasso. *Communications in Statistics-Simulation and Computation* 41(9), 1593–1605.

Kim, S. (2015). ppcor: An R package for a fast calculation to semi-partial correlation coefficients. *Communications for Statistical Applications and Methods* 22(6), 665.

Kropko, J. and J. H. Jeffrey (2019). coxed: An R package for computing duration-based quantities from the Cox proportional hazards model.

Kvamme, H., Ø. Borgan, and I. Scheel (2019). Time-to-event prediction with neural networks and Cox regression. *Journal of Machine Learning Research* 20(129), 1–30.

Lagani, V. and I. Tsamardinos (2010). Structure-based variable selection for survival data. *Bioinformatics* 26(15), 1887–1894.

Laimighofer, M., J. Krumsiek, F. Buettner, and F. J. Theis (2016). Unbiased prediction and feature selection in high-dimensional survival regression. *Journal of Computational Biology* 23(4), 279–290.

Lee, K. H., S. Chakraborty, J. Sun, et al. (2011). Bayesian variable selection in semiparametric proportional hazards model for high dimensional survival data. *The International Journal of Biostatistics* 7(1), 1–32.

Li, Y., B. Mark, G. Raskutti, R. Willett, H. Song, and D. Neiman (2020). Graph-based regularization for regression problems with alignment and highly correlated designs. *SIAM Journal on Mathematics of Data Science* 2(2), 480–504.

Murphy, S. A. and A. W. Van der Vaart (2000). On profile likelihood. *Journal of the American Statistical Association* 95(450), 449–465.

Murtaugh, P. A., E. R. Dickson, G. M. Van Dam, M. Malinchoc, P. M. Grambsch, A. L. Langworthy, and C. H. Gips (1994). Primary biliary cirrhosis: Prediction of short-term survival based on repeated patient visits. *Hepatology* 20(1), 126–134.

Newcombe, P. J., H. Raza Ali, F. M. Blows, E. Provenzano, P. D. Pharoah, C. Caldas, and S. Richardson (2017). Weibull regression with Bayesian variable selection to identify prognostic tumour markers of breast cancer survival. *Statistical Methods in Medical Research* 26(1), 414–436.

Nikooienejad, A., W. Wang, and V. E. Johnson (2020). Bayesian variable selection for survival data using inverse moment priors. *Annals of Applied Statistics* 14(2), 809.

Obozinski, G., L. Jacob, and J.-P. Vert (2011). Group lasso with overlaps: The latent group lasso approach. *arXiv preprint arXiv:1110.0413*.

Rennert, L. and S. X. Xie (2018). Cox regression model under dependent truncation. *arXiv preprint arXiv:1803.09830*.

Tachmazidou, I., M. R. Johnson, and M. De Iorio (2010). Bayesian variable selection for survival regression in genetics. *Genetic Epidemiology* 34(7), 689–701.

Terasaki, P. I., J. M. Cecka, D. W. Gjertson, and S. Takemoto (1995). High survival rates of kidney transplants from spousal and living unrelated donors. *New England Journal of Medicine* 333(6), 333–336.

Therneau, T. M., T. Lumley, A. Elizabeth, and C. Cynthia (2020). *Package ‘survival’: Survival Analysis*.

Tibshirani, R. (1996). Regression shrinkage and selection via the lasso. *Journal of the Royal Statistical Society: Series B (Methodological)* 58(1), 267–288.

Tibshirani, R. (1997). The lasso method for variable selection in the Cox model. *Statistics in Medicine* 16(4), 385–395.

Tibshirani, R., M. Saunders, S. Rosset, J. Zhu, and K. Knight (2005). Sparsity and smoothness via the fused lasso. *Journal of the Royal Statistical Society: Series B (Statistical Methodology)* 67(1), 91–108.

Utazirubanda, J. C., T. M. León, and P. Ngom (2019). Variable selection with group lasso approach: Application to Cox regression with frailty model. *Communications in Statistics-Simulation and Computation*, 1–21.

Walter, S. and H. Tiemeier (2009). Variable selection: Current practice in epidemiological studies. *European Journal of Epidemiology* 24(12), 733–736.

Wu, Y. (2012). Elastic net for Cox’s proportional hazards model with a solution path algorithm. *Statistica Sinica* 22, 27–294.

Yu, G. and Y. Liu (2016). Sparse regression incorporating graphical structure among predictors. *Journal of the American Statistical Association* 111(514), 707–720.

Yuan, M. and Y. Lin (2006). Model selection and estimation in regression with grouped variables. *Journal of the Royal Statistical Society: Series B (Statistical Methodology)* 68(1), 49–67.

Zhang, H. H. and W. Lu (2007). Adaptive lasso for Cox’s proportional hazards model. *Biometrika* 94(3), 691–703.

Zou, H. (2006). The adaptive lasso and its oracle properties. *Journal of the American Statistical Association* 101(476), 1418–1429.

Zou, H. and T. Hastie (2005). Regularization and variable selection via the elastic net. *Journal of the Royal Statistical Society: series B (Statistical Methodology)* 67(2), 301–320.

SUPPLEMENTARY MATERIAL

A Additional details on the numerical examples

Table 10: Connected variables and their neighbors in the *pbcsseq* dataset used in Section 6.2.

| Variable | Neighbors |
|----------|---------------------------------------|
| age | albumin, ast |
| bili | chol, albumin, ast, platelet, protime |
| chol | alk.phos, ast, platelet, protime |
| albumin | ast, platelet, protime |
| alk.phos | ast, platelet |
| ast | platelet |
| platelet | protime |
| edema0.5 | edema1 |
| stage2 | stage3, stage4 |

B Local approximation for partial likelihood function

For completeness, here we provide the method used in Andersen and Gill (1982); Fan and Li (2002) to express the log-likelihood function as a quadratic function in a $n^{-1/2}$ neighborhood of the true parameter β_0 . Recall that we have defined the counting process $N_i(t) = \mathbb{1}\{T_i \leq t, T_i \leq C_i\}$, $Y_i(t) = \mathbb{1}\{T_i \geq t, C_i \geq t\}$, and the partial likelihood equals to

$$\ell(\beta) = \sum_{i=1}^n \int_0^1 \beta^\top \mathbf{x}_i(s) dN_i(s) - \int_0^1 \log \left\{ \sum_{i=1}^n Y_i(s) \exp\{\beta^\top \mathbf{x}_i(s)\} \right\} d\bar{N}(s),$$

where $\bar{N} = \sum_{i=1}^n N_i$.

Under Assumptions 1, for each β in a neighborhood \mathcal{B} of β_0 , we have (Andersen and

Gill, 1982):

$$\begin{aligned} \frac{1}{n} \{ \ell(\boldsymbol{\beta}) - \ell(\boldsymbol{\beta}_0) \} &= \int_0^1 \left[(\boldsymbol{\beta} - \boldsymbol{\beta}_0)^\top s^{(1)}(\boldsymbol{\beta}_0, t) - \log \left\{ \frac{s^{(0)}(\boldsymbol{\beta}, t)}{s^{(0)}(\boldsymbol{\beta}_0, t)} \right\} s^{(0)}(\boldsymbol{\beta}_0, t) \right] h_0(t) dt \\ &\quad + O_P\left(\frac{\|\boldsymbol{\beta} - \boldsymbol{\beta}_0\|}{\sqrt{n}}\right). \end{aligned}$$

Note that the first-order derivative of the first term on the right hand side equals to 0 at $\boldsymbol{\beta}_0$. By Taylor's expansion, we have

$$\frac{1}{n} \{ \ell(\boldsymbol{\beta}) - \ell(\boldsymbol{\beta}_0) \} = -\frac{1}{2} (\boldsymbol{\beta} - \boldsymbol{\beta}_0)^\top \{ I(\boldsymbol{\beta}_0) + o_P(1) \} (\boldsymbol{\beta} - \boldsymbol{\beta}_0) + O_P(n^{-1/2} \|\boldsymbol{\beta} - \boldsymbol{\beta}_0\|). \quad (11)$$

Define the scaled objective function with regularization as $\mathcal{L}(\boldsymbol{\beta}) = -\ell(\boldsymbol{\beta}) + n\lambda \|\boldsymbol{\beta}\|_{G,\tau}$. For $\alpha_n > 0$, if we can show that for any given $\epsilon > 0$, there exists a large constant $C > 0$ such that

$$\mathbb{P} \left\{ \inf_{\|\boldsymbol{u}\|=C} \mathcal{L}(\boldsymbol{\beta}_0 + \alpha_n \boldsymbol{u}) > \mathcal{L}(\boldsymbol{\beta}_0) \right\} \geq 1 - \epsilon,$$

then this implies that with probability at least $1 - \epsilon$ there exists a local minima in the ball $\{\boldsymbol{\beta}_0 + \alpha_n \boldsymbol{u} : \|\boldsymbol{u}\| \leq C\}$. Hence, there exists a local minimizer such that $\|\widehat{\boldsymbol{\beta}} - \boldsymbol{\beta}_0\| = O_P(\alpha_n)$. To show this, we first note that

$$\frac{1}{n} \{ \mathcal{L}(\boldsymbol{\beta}_0) - \mathcal{L}(\boldsymbol{\beta}_0 + \alpha_n \boldsymbol{u}) \} = \frac{1}{n} \{ \ell(\boldsymbol{\beta}_0 + \alpha_n \boldsymbol{u}) - \ell(\boldsymbol{\beta}_0) \} - \lambda [\|\boldsymbol{\beta}_0 + \alpha_n \boldsymbol{u}\|_{G,\tau} - \|\boldsymbol{\beta}_0\|_{G,\tau}]. \quad (12)$$

By (11), we have:

$$\frac{1}{n} \{ \ell(\boldsymbol{\beta}_0 + \alpha_n \boldsymbol{u}) - \ell(\boldsymbol{\beta}_0) \} = -\frac{1}{2} \alpha_n^2 \boldsymbol{u}^\top \{ I(\boldsymbol{\beta}_0) + o_P(1) \} \boldsymbol{u} + O_P(n^{-1/2} \alpha_n \|\boldsymbol{u}\|).$$

The first term is of the order $O(\alpha_n^2 C^2)$, and the second term is of the order $O(n^{-1/2} \alpha_n C)$.

For the regularization term, since $\|\boldsymbol{\beta}_0 + \alpha_n \boldsymbol{u}\|_{G,\tau} \geq \|\boldsymbol{\beta}_0\|_{G,\tau} - \alpha_n \|\boldsymbol{u}\|_{G,\tau}$, we have

$$-\lambda [\|\boldsymbol{\beta}_0 + \alpha_n \boldsymbol{u}\|_{G,\tau} - \|\boldsymbol{\beta}_0\|_{G,\tau}] \leq \lambda \alpha_n \|\boldsymbol{u}\|_{G,\tau}.$$

If the term $O(\alpha_n^2 C^2)$ dominates the whole expression (12) (which is possible by choosing a sufficiently large constant C), then we have that there exists a local minimizer $\widehat{\boldsymbol{\beta}}$ of $\mathcal{L}(\boldsymbol{\beta})$ that is close to true parameter in the sense that $\|\widehat{\boldsymbol{\beta}} - \boldsymbol{\beta}_0\| = O_P(\alpha_n)$.

C Proofs

We first introduce a lemma that will be frequently used in the following.

Lemma 1 (Yu and Liu (2016)). *For any predictor graph G and positive weights τ_i , suppose $V^{(1)}, V^{(2)}, \dots, V^{(p)}$ is an optimal decomposition of $\beta \in \mathbb{R}^p$, then for any $S \subseteq \{1, 2, \dots, p\}$, $\{V^{(j)}, j \in S\}$ is also an optimal decomposition of $\sum_{j \in S} V^{(j)}$.*

Proof of Theorem 1. Suppose $\widehat{\beta}$ is the optimal solution to the regularization problem, then for any $\beta \in \mathbb{R}^p$, we have

$$-\frac{1}{n} \ell(\widehat{\beta}) + \lambda \|\widehat{\beta}\|_{G, \tau} \leq -\frac{1}{n} \ell(\beta) + \lambda \|\beta\|_{G, \tau}.$$

Let $\beta = \beta_0$, we have

$$\frac{1}{n} \left\{ \ell(\beta_0) - \ell(\widehat{\beta}) \right\} \leq \lambda \left(\|\beta_0\|_{G, \tau} - \|\widehat{\beta}\|_{G, \tau} \right). \quad (13)$$

Let $\{S^{(1)}, S^{(2)}, \dots, S^{(p)}\} \in \mathcal{U}(\beta_0)$ be an arbitrary optimal decomposition of β_0 , and let $\{T^{(1)}, T^{(2)}, \dots, T^{(p)}\} \in \mathcal{U}(\widehat{\beta} - \beta_0)$ be an arbitrary optimal decomposition of $\widehat{\beta} - \beta_0$. We have $\widehat{\beta} - \beta_0 = \sum_{i=1}^p T^{(i)}$. Thus, by (11) we have:

$$\begin{aligned} \frac{1}{n} \left\{ \ell(\widehat{\beta}) - \ell(\beta_0) \right\} &= -\frac{1}{2} (\widehat{\beta} - \beta_0)^\top \{I(\beta_0) + o_P(1)\} (\widehat{\beta} - \beta_0) + O_P(n^{-1/2} \|\widehat{\beta} - \beta_0\|) \\ &= -\frac{1}{2} \left(\sum_{i=1}^p T^{(i)} \right)^\top \{I(\beta_0) + o_P(1)\} \left(\sum_{i=1}^p T^{(i)} \right) + O_P(n^{-1/2} \left\| \sum_{i=1}^p T^{(i)} \right\|). \end{aligned} \quad (14)$$

By Assumption 2 (1), we can choose $S^{(j)} = 0, \forall j \in J_0^c$, thus $\beta_0 = \sum_{j \in J_0} S^{(j)}$, and

$$\begin{aligned} \|\widehat{\beta}\|_{G, \tau} &= \|\widehat{\beta} - \beta_0 + \beta_0\|_{G, \tau} \\ &= \left\| \sum_{j \in J_0} T^{(j)} + \sum_{j \notin J_0} T^{(j)} + \sum_{j \in J_0} S^{(j)} \right\|_{G, \tau} \\ &\geq \left\| \sum_{j \notin J_0} T^{(j)} + \sum_{j \in J_0} S^{(j)} \right\|_{G, \tau} - \left\| \sum_{j \in J_0} T^{(j)} \right\|_{G, \tau} \\ &= \left\| \sum_{j \notin J_0} T^{(j)} \right\|_{G, \tau} + \left\| \sum_{j \in J_0} S^{(j)} \right\|_{G, \tau} - \left\| \sum_{j \in J_0} T^{(j)} \right\|_{G, \tau}. \end{aligned}$$

Note that $\|\sum_{j \in J_0} S^{(j)}\|_{G, \tau} = \|\beta_0\|_{G, \tau}$, thus

$$\|\beta_0\|_{G, \tau} - \|\widehat{\beta}\|_{G, \tau} \leq \left\| \sum_{j \in J_0} T^{(j)} \right\|_{G, \tau} - \left\| \sum_{j \notin J_0} T^{(j)} \right\|_{G, \tau}.$$

Combining with (13) and note that the left-hand side of (13) is non-negative, we have

$$\left\| \sum_{j \notin J_0} T^{(j)} \right\|_{G, \tau} \leq \left\| \sum_{j \in J_0} T^{(j)} \right\|_{G, \tau}. \quad (15)$$

Moreover, we have

$$\|\beta_0\|_{G, \tau} - \|\widehat{\beta}\|_{G, \tau} \leq \left\| \sum_{j \in J_0} T^{(j)} \right\|_{G, \tau} - \left\| \sum_{j \notin J_0} T^{(j)} \right\|_{G, \tau} \leq \left\| \sum_{j \in J_0} T^{(j)} \right\|_{G, \tau} = \sum_{j \in J_0} \tau_j \|T^{(j)}\|_2,$$

where the last equality is by Lemma 1. By the definition of $K_{G, \tau}$, we can select $\{T^{(1)}, \dots, T^{(p)}\}$ such that there are at most $K_{G, \tau}$ nonzero $T^{(j)}$'s, by (13) we have:

$$\frac{1}{n} \left\{ \ell(\beta_0) - \ell(\widehat{\beta}) \right\} \leq \lambda \sum_{j \in J_0} \tau_j \|T^{(j)}\|_2 \leq \lambda K_{G, \tau}^{1/2} \sqrt{\sum_{j \in J_0} \tau_j^2 \|T^{(j)}\|_2^2}.$$

On the other hand, from the Assumption 2 (2), (15), and (14), we have:

$$\frac{1}{n} \left\{ \ell(\beta_0) - \ell(\widehat{\beta}) \right\} \geq \kappa \sum_{j \in J_0} \tau_j^2 \|T^{(j)}\|_2^2.$$

Combine with the aforementioned equation, we have

$$\frac{1}{n} \left\{ \ell(\beta_0) - \ell(\widehat{\beta}) \right\} \leq \lambda K_{G, \tau}^{1/2} \sqrt{\sum_{j \in J_0} \tau_j^2 \|T^{(j)}\|_2^2} \leq \frac{\lambda K_{G, \tau}^{1/2}}{\sqrt{\kappa}} \sqrt{\frac{1}{n} \left\{ \ell(\beta_0) - \ell(\widehat{\beta}) \right\}},$$

which translates into the following:

$$\frac{1}{n} \left\{ \ell(\beta_0) - \ell(\widehat{\beta}) \right\} \leq \frac{\lambda^2 K_{G, \tau}}{\kappa}.$$

Furthermore,

$$\begin{aligned} \|\widehat{\beta} - \beta_0\|_2 &= \left\| \sum_{j=1}^p T^{(j)} \right\|_2 \leq \frac{\|\widehat{\beta} - \beta_0\|_{G, \tau}}{\tau_{\min}} = \frac{\sum_{j \in J_0} \tau_j \|T^{(j)}\|_2 + \sum_{j \notin J_0} \tau_j \|T^{(j)}\|_2}{\tau_{\min}} \\ &\leq \frac{2 \sum_{j \in J_0} \tau_j \|T^{(j)}\|_2}{\tau_{\min}} \leq \frac{2 K_{G, \tau}^{1/2}}{\sqrt{\kappa} \tau_{\min}} \cdot \sqrt{\frac{1}{n} \left\{ \ell(\beta_0) - \ell(\widehat{\beta}) \right\}} \\ &\leq \frac{2 \lambda K_{G, \tau}}{\kappa \tau_{\min}}. \end{aligned}$$

□

Proof to Theorem 2. For each $\mathbf{u} \in \mathbb{R}^p$, define

$$Q_n(\mathbf{u}) = -\ell(\boldsymbol{\beta}_0 + n^{-1/2}\mathbf{u}) + n\lambda\|\boldsymbol{\beta}_0 + n^{-1/2}\mathbf{u}\|_{G,\tau}.$$

Since $\widehat{\boldsymbol{\beta}}$ is the maximum penalized likelihood estimate, we define

$$\hat{\mathbf{u}} := \sqrt{n}(\widehat{\boldsymbol{\beta}} - \boldsymbol{\beta}_0) = \arg \min_{\mathbf{u} \in \mathbb{R}^p} Q_n(\mathbf{u}).$$

We also have

$$\begin{aligned} Q_n(\mathbf{u}) - Q_n(0) &= \ell(\boldsymbol{\beta}_0) - \ell(\boldsymbol{\beta}_0 + n^{-1/2}\mathbf{u}) + n\lambda(\|\boldsymbol{\beta}_0 + n^{-1/2}\mathbf{u}\|_{G,\tau} - \|\boldsymbol{\beta}_0\|_{G,\tau}) \\ &= \frac{1}{2}\mathbf{u}^\top I(\boldsymbol{\beta}_0)\mathbf{u} + o_P(1) + n\lambda(\|\boldsymbol{\beta}_0 + n^{-1/2}\mathbf{u}\|_{G,\tau} - \|\boldsymbol{\beta}_0\|_{G,\tau}). \end{aligned}$$

For the second term, we have

$$\|\boldsymbol{\beta}_0 + n^{-1/2}\mathbf{u}\|_{G,\tau} - \|\boldsymbol{\beta}_0\|_{G,\tau} = \|(\boldsymbol{\beta}_0 + n^{-1/2}\mathbf{u})_{J_0}\|_{G,\tau} - \|\boldsymbol{\beta}_0\|_{G,\tau} + \|(n^{-1/2}\mathbf{u})_{J_0^c}\|_{G,\tau}.$$

Suppose $V^{(1)}, \dots, V^{(p)}$ is an optimal decomposition of \mathbf{u} , then we have

$$n\lambda(\|(\boldsymbol{\beta}_0 + n^{-1/2}\mathbf{u})_{J_0}\|_{G,\tau} - \|\boldsymbol{\beta}_0\|_{G,\tau}) \leq \sqrt{n}\lambda \sum_{j \in J_0} \tau_j \|V^{(j)}\|_2.$$

If $\sqrt{n}\lambda \rightarrow 0$ and $\tau_j = O(1)$ for each $j \in J_0$, then for each fixed \mathbf{u} , we have

$$n\lambda(\|(\boldsymbol{\beta}_0 + n^{-1/2}\mathbf{u})_{J_0}\|_{G,\tau} - \|\boldsymbol{\beta}_0\|_{G,\tau}) \rightarrow 0, \text{ as } n \rightarrow \infty. \quad (16)$$

If $n^{(\gamma+1)/2}\lambda \rightarrow \infty$, $\mathbf{u}_{J_0^c} \neq 0$, and $\liminf_{n \rightarrow \infty} n^{-\gamma/2}\tau_j > 0$ for each $j \in J_0^c$, then

$$n\lambda\|(n^{-1/2}\mathbf{u})_{J_0^c}\|_{G,\tau} = \sqrt{n}\lambda \sum_{j \in J_0^c} \tau_j \|V^{(j)}\|_2 = n^{(\gamma+1)/2}\lambda \cdot n^{-\gamma/2} \sum_{j \in J_0^c} \tau_j \|V^{(j)}\|_2 \rightarrow \infty. \quad (17)$$

Combining (16) and (17), we have:

$$Q_n(\mathbf{u}) - Q_n(0) \xrightarrow{d} \begin{cases} \ell(\boldsymbol{\beta}_0) - \ell(\boldsymbol{\beta}_0 + n^{-1/2}\mathbf{u}) & \text{if } \text{supp}(\mathbf{u}) \subset J_0, \\ \infty & \text{o.w.} \end{cases}$$

This implies that

$$\widehat{\boldsymbol{\beta}}_{J_0^c} \xrightarrow{d} 0.$$

We note that $\hat{\mathbf{u}} = \arg \min Q_n(\mathbf{u}) = \arg \min \{Q_n(\mathbf{u}) - Q_n(0)\}$, thus it suffices to show that the $\hat{\mathbf{u}} = \arg \max_{\text{supp}(\mathbf{u}) \subset J_0} l(\boldsymbol{\beta}_0 + n^{-1/2}\mathbf{u})$ is asymptotically normal distributed. To prove this, denote the first-order derivative of the partial log-likelihood with respect to $\boldsymbol{\beta}$ as

$$U(\boldsymbol{\beta}) = \sum_{i=1}^n \int_0^1 \mathbf{x}_i(t) dN_i(t) - \int_0^1 \frac{\sum_{i=1}^n Y_i(t) \mathbf{x}_i(t) \exp\{\boldsymbol{\beta}^\top \mathbf{x}_i(t)\}}{\sum_{i=1}^n Y_i(t) \exp\{\boldsymbol{\beta}^\top \mathbf{x}_i(t)\}} d\bar{N}(t).$$

And the second-order derivative as

$$S(\boldsymbol{\beta}) = - \int_0^1 \left(\frac{\sum_{i=1}^n Y_i(t) \mathbf{x}_i(t) \mathbf{x}_i(t)^\top \exp\{\boldsymbol{\beta}^\top \mathbf{x}_i(t)\}}{\sum_{i=1}^n Y_i(t) \exp\{\boldsymbol{\beta}^\top \mathbf{x}_i(t)\}} - \frac{[\sum_{i=1}^n Y_i \mathbf{x}_i(t) \exp\{\boldsymbol{\beta}^\top \mathbf{x}_i(t)\}][\sum_{i=1}^n Y_i(t) \mathbf{x}_i(t) \exp\{\boldsymbol{\beta}^\top \mathbf{x}_i(t)\}]^\top}{[\sum_{i=1}^n Y_i(t) \exp\{\boldsymbol{\beta}^\top \mathbf{x}_i(t)\}]^2} \right) d\bar{N}(t).$$

Using taylor expansion, we have

$$U(\hat{\boldsymbol{\beta}}) - U(\boldsymbol{\beta}_0) = S(\boldsymbol{\beta}^*)(\hat{\boldsymbol{\beta}} - \boldsymbol{\beta}_0),$$

where $\boldsymbol{\beta}^*$ is on the line segment between $\hat{\boldsymbol{\beta}}$ and $\boldsymbol{\beta}_0$, and $-S(\boldsymbol{\beta})$ is a positive semidefinite matrix. By Theorem 3.2 in Andersen and Gill (1982), we have

$$\frac{1}{\sqrt{n}} U_{J_0}(\boldsymbol{\beta}_0) \xrightarrow{d} N(0, I_{J_0}(\boldsymbol{\beta}_0)), \quad -\frac{1}{n} S(\boldsymbol{\beta}^*) \xrightarrow{p} I_{J_0}(\boldsymbol{\beta}_0), \quad \text{as } n \rightarrow \infty,$$

where $U_{J_0}(\boldsymbol{\beta}_0)$ consists of the elements of $U(\boldsymbol{\beta}_0)$ with index belonging to the set J_0 , and $I_{J_0}(\boldsymbol{\beta}_0)$ is a square matrix with rows and columns belong to the index set J_0 . Since $U(\hat{\boldsymbol{\beta}}) = 0$, we have $-S(\boldsymbol{\beta}^*)(\hat{\boldsymbol{\beta}} - \boldsymbol{\beta}_0) = U(\boldsymbol{\beta}_0)$, thus by Slutsky's Theorem, we have

$$\sqrt{n} I_{J_0}(\boldsymbol{\beta}_0)(\hat{\boldsymbol{\beta}}_{J_0} - \boldsymbol{\beta}_{0,J_0}) \xrightarrow{d} N(0, I_{J_0}(\boldsymbol{\beta}_0)),$$

which translates into

$$\sqrt{n}(\hat{\boldsymbol{\beta}}_{J_0} - \boldsymbol{\beta}_{0,J_0}) \xrightarrow{d} N(0, I_{J_0}(\boldsymbol{\beta}_0)^{-1}).$$

□